Microelectromechanical Deformable Mirrors

Thomas G. Bifano, Julie Perreault, Raji Krishnamoorthy Mali, and Mark N. Horenstein

Abstract— **A new class of silicon-based deformable mirrors is described. These devices are capable of correcting time-varying aberrations in imaging or beam forming applications. Each mirror is composed of a flexible silicon membrane supported by an underlying array of electrostatic parallel plate actuators. All structural and electronic elements were fabricated through conventional surface micromachining using polycrystalline silicon thin films. A layout and fabrication design strategy for reducing nonplanar topography in multilayer micromachining was developed and used to achieve nearly flat membrane surfaces. Several deformable mirrors were characterized for their electromechanical performance. Real-time correction of optical aberrations was demonstrated using a single mirror segment connected to a closed-loop feedback control system. Undesirable mirror contours caused by residual stress gradients in the membrane were observed.**

Index Terms— **Adaptive optics, microelectromechanical devices, mirrors, optical phase conjugation.**

I. Introduction

A DEFORMABLE mirror in combination with a wavefront sensor and real-time controller can be used to modulate the spatial phase of an optical wavefront. Such phase modulation is often termed "adaptive optics" and has found its most frequent and successful application in large-aperture astronomical telescopes, where it is used to compensate for optical aberrations introduced by atmospheric turbulence. Most deformable mirrors (DM's) that are commercially available today are macroscopic devices made with flat glass mirror plates supported by an array of piezoelectric actuators. Recent additions to the collection of DM devices include bulk micromachined modal mirrors [1] and [2] and surface micromachined, piston motion segmented mirrors [3]. In this paper, the first continuous membrane zonal DM's fabricated as microelectromechanical systems (MEMS) are introduced and discussed in detail. MEMS-based segmented mirrors (both piston and tip-tilt) having fill factors in the range of 95%–98% are also described.

Deformable mirrors (DM's) based on MEMS technology hold the promise of an inexpensive low-power compact high-performance alternative to existing designs. The emergence of MEMS-based deformable mirrors is likely to extend the field of adaptive optics from its roots in astronomical imaging systems to the commercially important areas of laser-based communications, biomedical imaging, laser welding, and terrestrial imaging.

Manuscript received August 5, 1998. This work was supported in part by the Defense Advanced Research Projects Agency, Electronics Technology Office, under Contract DABT63-95-C-0065.

The authors are with the College of Engineering, Aerospace and Mechanical Engineering, Boston University, Boston, MA 02215 USA.

Publisher Item Identifier S 1077-260X(99)01962-0.

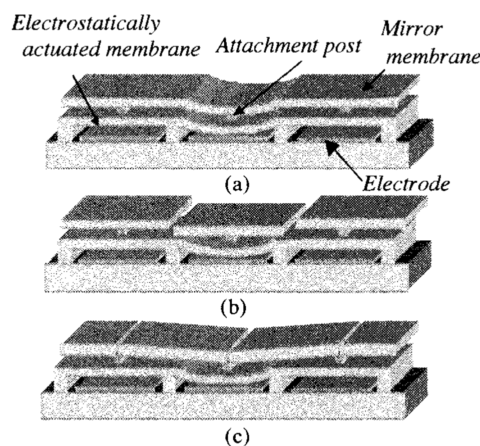

Fig. 1. Schematic of deformable mirror array sections with: (a) continuous mirrors, (b) segmented mirrors with piston motion, and (c) segmented mirrors having tip-tilt motion (not to scale).

A variety of MEMS-based deformable mirrors have been investigated by other research groups. In the research reported here, three types of mirror systems have been investigated. They are depicted in schematic form in Fig. 1. In each type, the 2-μm-thick mirror membranes are supported by an underlying array of identical electrostatic actuators. Mirrors are attached to actuators via small, 3-μm-long attachment posts. The typical actuator consists of a 300 $\times$ 300 $\times$ 2 μm polycrystalline silicon layer anchored to a substrate along two opposite edges. The actuator membrane serves as the upper electrode of a parallel plate capacitor. A lower, stationary pad of polycrystalline silicon was deposited over an electrically insulating 0.5-μm-thick silicon nitride layer that covers the silicon substrate. This pad serves as the other capacitor electrode. Applying a voltage between the lower capacitor electrode and the grounded upper actuator membrane causes the latter to deflect downward, in turn moving its 3-μm post and point of attachment to the mirror. An air–gap, typically 5 μm thick, separates the actuator membrane from its voltage activation pad.

Continuous membrane mirrors [Fig. 1(a)] have the advantage that they cause almost no diffraction of the reflected beam. Such membranes also ensure smooth and continuous phase variations across the mirror.

Mechanical coupling occurs between actuators because of their common attachment to the mirror membrane. The resulting interactuator "influence function" complicates the adaptive-optic control problem. In adaptive optics, a compromise must be made between ensuring phase continuity and reducing interactuator coupling in DM's. Generally, an influence function of about 10% between adjacent actuators is chosen, and this value was used as a target for the continuous

1077–260X/99$10.00 © 1999 IEEE

mirrors developed in this research. In MEMS-DM's, the influence function can be varied over a wide range by adjusting the ratio of mechanical compliance of the actuator membrane to that of the mirror membrane.

Segmented mirrors [Fig. 1(b)], capable of pure piston motion only, provide one alternative to continuous mirror devices. They exhibit no interactuator coupling but may produce undesirable diffraction due to the gaps between adjacent segments. Also, they do not permit spatially continuous phase modulation across the face of the mirror.

Hybrid mirror designs that permit tip-tilt motion in addition to piston motion [Fig. 1(c)] allow optical phase to be matched at the interface between adjacent mirror segments. This feature ensures phase continuity across the entire mirror face. Tip-tilt mirrors exhibit some diffraction and interactuator coupling. Both segmented and tip-tilt mirrors allow relief of biaxial in-plane components of residual stress (i.e., average tension or compression) in the mirror membrane upon structural release. Such stresses are frequently problematic in surface micromachined devices.

The primary variables of interest in an adaptive optics system are the number of actuators in the DM, the motion resolution of each segment, the control bandwidth of each actuator, and the maximum available actuator stroke. Design goals for our MEMS-DM system were determined based on the requirements of a typical astronomical telescope imaging system. Our goal has been to build a DM having 100 electrostatic actuators, 2-μm stroke per actuator, 10-nm resolution, 1-kHz open loop bandwidth, and 1-cm^2 total active mirror area.

II. Device Fabrication

Prototype actuators and mirror systems were first fabricated in a multiuser three-layer polysilicon foundry process offered by MCNC (MUMPS) [4]. A detailed study of electrostatic actuators fabricated in MUMPS previously reported [5] indicated a device yield that was sufficient (~95%) to make large-scale mirror arrays feasible. Statistical analysis of an ensemble of ramp actuation tests on these actuators revealed a position repeatability of 10 nm for standard deviation limits corresponding to 99% probability. A dynamic motion response study showed the actuators to have a mechanical response frequency bandwidth of at least 70 kHz. Some electrostatic charging effects were observed, possibly due to the presence of surface leakage paths [6].

The first deformable mirrors produced had excessive surface topography caused by the patterning and etching of successive structural and sacrificial films. A novel layout strategy for reducing nonplanar topography in multilayer micromachining was developed to overcome this problem. By restricting the maximum spacing between features (i.e., the width of etch lines) on all patterned layers, it was possible to reduce the surface topography to submicron levels. Restricting the etched spaces to the minimum achievable values (1.5 μm for MUMPS) allows subsequent conformal layers to rapidly fill those spaces, reducing undesired topography. Where wide anchors are desired, they are fabricated by joining many narrow features into a honeycomb pattern. If no etch access holes are provided on the interior of such honeycomb structures, the solid oxide interior remains as a structural component in the planar, honeycomb anchor. Using this planarization strategy, a number of prototype continuous MEMS-DM's were fabricated using the MUMPS foundry process. Experimental and modeling results for these mirrors have been reported previously [7].

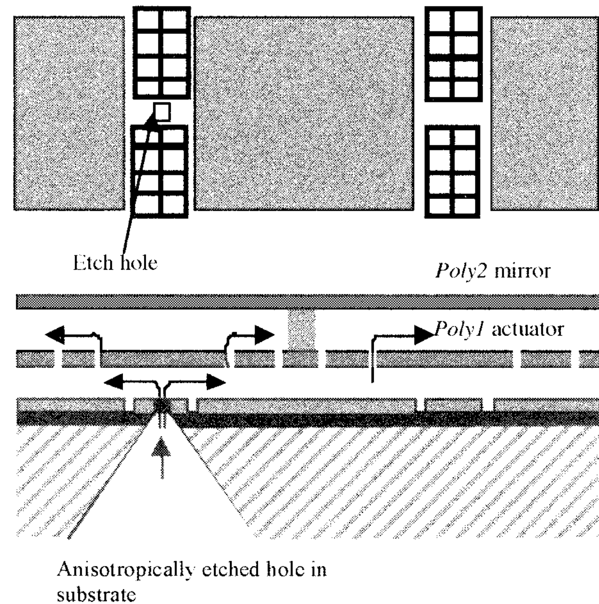

Fig. 2. Backside etch access holes for release etching without adding holes to the continuous mirror membrane.

The major limitation in using the MCNC MUMPS fabrication process for creating DM devices is the small amount of vertical actuator stroke that can be achieved. In MUMPS, the first sacrificial oxide film (2 μm thick) eventually forms the electrostatic gap of the actuator. The well-known electromechanical "snap through," or pull-in instability of parallel plate electrostatic actuators limits the useful stroke of the actuator to a little more than one third of the total gap spacing. This phenomenon limits the useful vertical stroke of a MUMPS actuator to about 700 nm. In an adaptive optics application involving visible light, actuator stroke of several micrometers is required for adequate performance.

Longer-stroke MEMS devices were fabricated at MCNC using a custom-defined fabrication process. The main goal of the custom process was to obtain a useful stroke of at least 2 μm. Obtaining this stroke required actuators having at least 5-μm gap spacing. A secondary goal was to develop a fabrication process that did not require etch holes on the mirror surface. Etch holes are normally required in surface micromachining to allow access to sacrificial oxide layers by buffered oxide etchants. As an alternative, an anisotropic etch was used to pattern a series of holes through the back side of the wafer, allowing the buffered oxide etchant to be carried to the sacrificial layers without the need for surface etch holes in the mirror layer. This concept is illustrated in Fig. 2. Some devices were fabricated in the custom run without anisotropic etch holes. For those devices, surface layer etch holes were patterned sparsely on the membrane mirror surface.

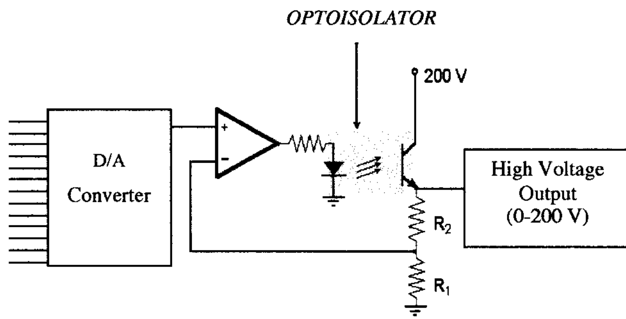

Fig. 3. Single channel of the electrostatic actuator drive circuit.

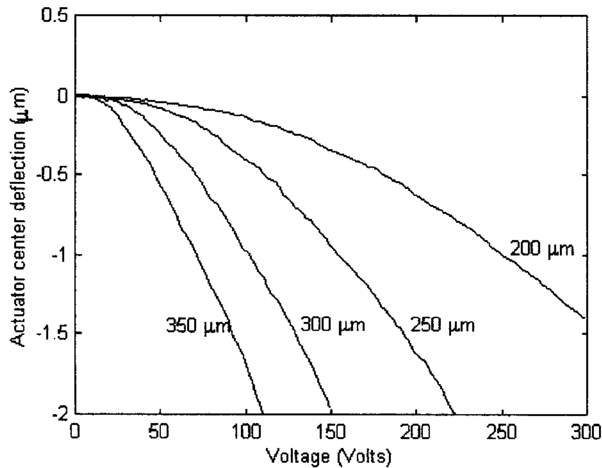

Fig. 4. Measured actuator deflection versus excitation voltage for square membrane electrostatic actuators. Actuator span is noted on the graph for each of four actuators tested. Actuator gap is 5 μm.

An electrostatic driver and control system was developed. This circuit was designed to be a low-cost amplifier that was easy to replicate in a multichannel MEMS mirror controller. Details of a single-actuator channel of the circuit are shown in Fig. 3. A parallel-encoded digital signal is transferred from the control computer to a latched digital-to-analog converter, which outputs a low-level analog voltage. The low-voltage signal, buffered by the operational amplifier, drives the light-emitting diode (LED) of an optoisolator. The phototransistor inside the optoisolator forces current into a resistive divider, providing feedback to the opamp. The current level through the phototransistor increases until the inverting op-amp input reaches nearly the same voltage as the noninverting input.

Several sets of actuators and mirrors were made using the custom fabrication process and were tested using various characterization tools. Stroke and mechanical frequency response of individual actuators were measured using a single point, split-frequency, displacement-measuring laser interferometer. This device uses a focused laser beam to measure surface-normal displacement to a position resolution of 2.5 nm and frequency bandwidth of up to 133 kHz. A useful stroke of 2 μm indeed was achieved on actuators with 5 μm actuator membrane-to-substrate gap spacing. Frequency response measurements showed usable mechanical bandwidths of at least 70 kHz for 1-μm stroke excursions of the actuators. This bandwidth is reduced by the addition of the continuous mirror membrane to approximately 3.5 kHz.

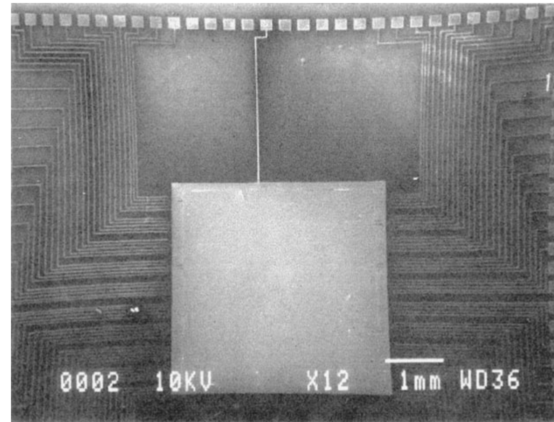

Fig. 5. SEM micrograph of a continuous mirror membrane supported by a 10 $\times$ 10 actuator array.

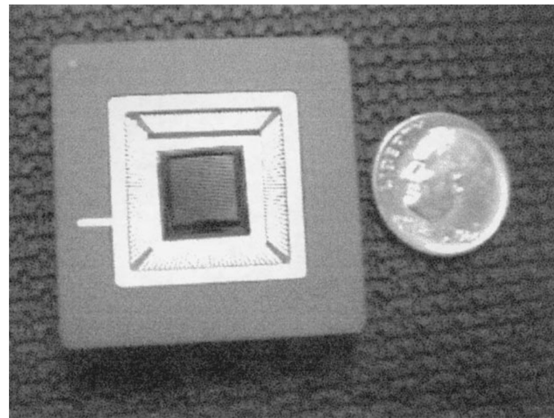

Fig. 6. Photo of a packaged continuous mirror supported by a 20 $\times$ 20 array of actuators.

The measured voltage-deflection curves for square actuators of various sizes are plotted in Fig. 4. The usable range of deflection for these actuators before electrostatic pull-in is 2 μm.

Fig. 5 shows a scanning electronic micrograph (SEM) of a continuous mirror supported by 100 actuators. A photo of a continuous mirror supported by a 20 $\times$ 20 array of 400 actuators is shown in Fig. 6. The device is mounted in a ceramic package measuring 35 $\times$ 35 $\times$ 6 mm.

The surface planarity of the mirror was measured using an interferometric microscope. Measurements showed a post release surface-normal deformation of approximately 50 nm (peak-to-valley) on the mirror surface when no voltage was applied to any actuator. This initial static deformation was thought to be caused by residual stress gradients in the thin film polysilicon membrane.

A surface map a cross-sectional surface profile of a continuous mirror before deflection of any actuators are shown in Fig. 7(a) and (b). The mirror size is 780 $\times$ 780 $\times$ 2 μm and it is supported by a 3 $\times$ 3 array of actuators via post attachments at the mirror corners, midway along each mirror

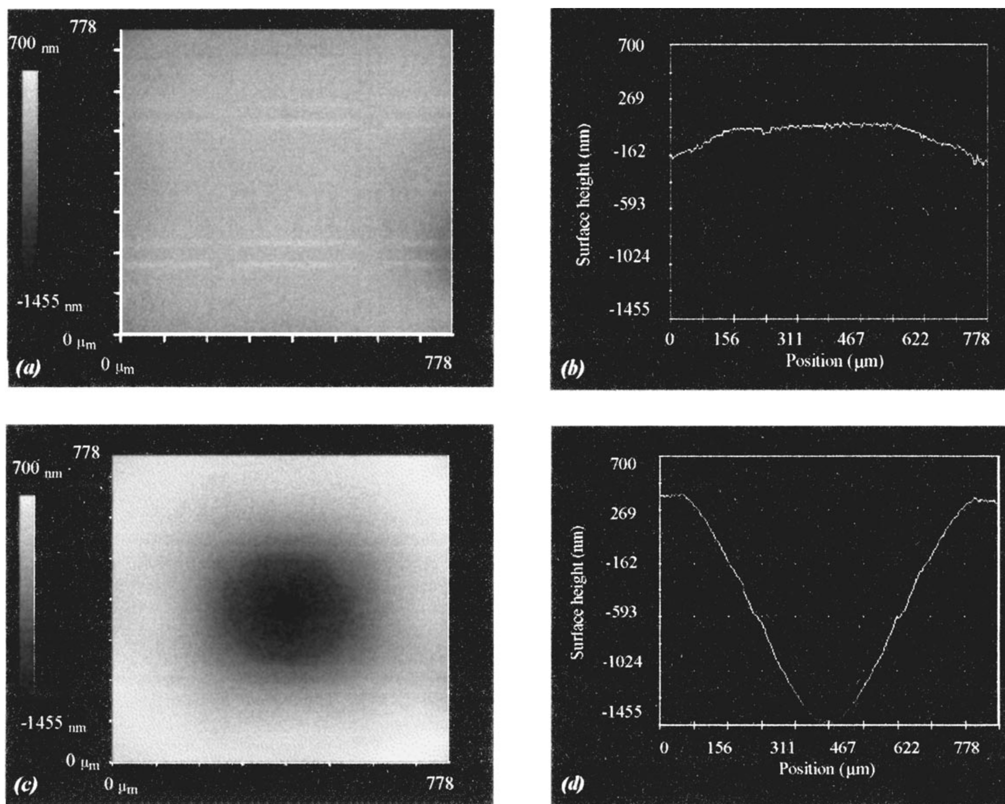

Fig. 7. (a), (c) Surface maps and (b), (d) through the center of a nine-element continuous mirror. Top: Unactuated. Bottom: Center actuator energized to 155 V. These measurements were made using an interfaerometric microscope.

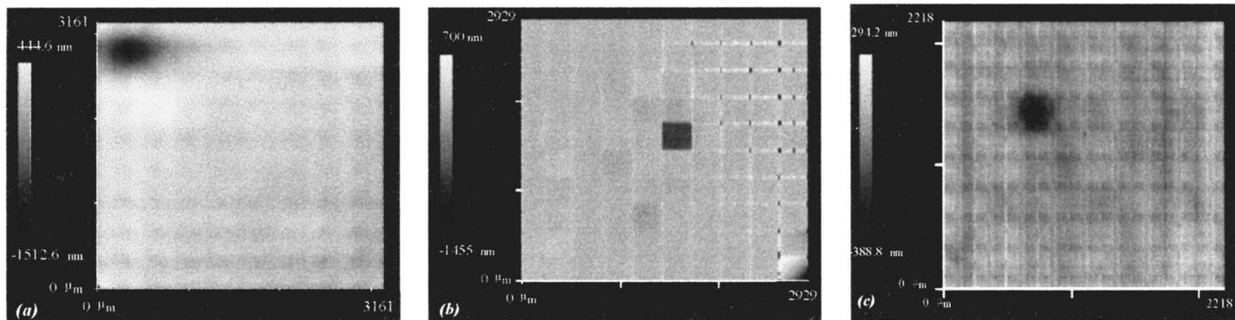

Fig. 8. Interferometric surface maps of 10 $\times$ 10 actuator arrays with: (a) continuous mirror, (b) segmented mirrors with piston motion, and (c) segmented mirrors with tip-tilt motion. All mirrors arrays measure approximately 4 mm on a side. In each case a single actuator has been deflected.

edge, and at the mirror center. Fig. 7(c) and (d) shows the same measurements after deflection of the center actuator.

Fig. 8 shows interferometric surface maps of all three deformable mirror designs in a 10 $\times$ 10 actuator configuration with local deflection caused by a single actuator. In these surface maps, darker color indicates that the surface has been pulled down. Note that significant coupling between actuators occurs in the continuous and hybrid tip-tilt mirrors because they are mechanically coupled through the mirror membrane. This coupling results in a smooth influence function in the neighborhood of the deflected actuator. The influence function (i.e., the ratio of deflection of an energized actuator to that of an unenergized neighbor) was measured to be about 10% for these devices. In the case of the segmented piston mirror, no interactuator coupling occurs, resulting in sharp phase transitions at the boundaries of the actuated segment.

Experiments also were performed on 10 $\times$ 10 continuous membrane mirrors to test their ability to generate optically interesting and useful surface shapes. Fig. 9, for example, shows a convex dome shape. A schematic cross section is depicted in Fig. 9(a), while Fig. 9(b) shows the measured surface profile of the continuous mirror device. All 100 support actuators were individually energized with appropriate voltages to impose the dome shape on the mirror. The measured height difference between the top of the dome and its lowest rim was about 1 μm.

To assess the optical and reflective quality of the polysilicon mirror surfaces, their small scale, local surface roughness

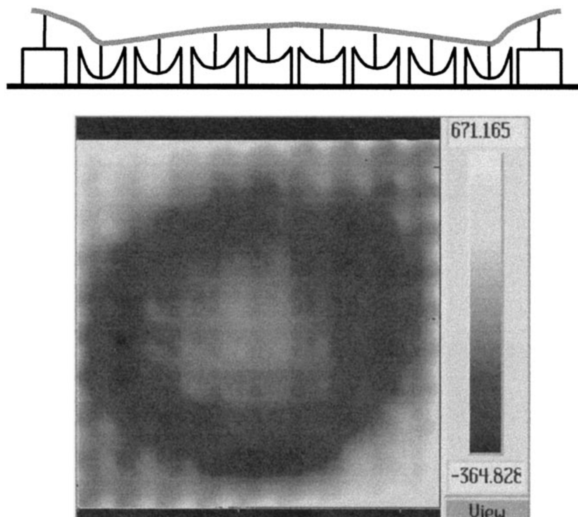

Fig. 9. Complex interior dome shape achieved with 10 × 10 zone continuous membrane MEMS-DM. Mirror membrane dimensions are 3 mm × 3 mm × 2 μm.

was measured using an atomic force microscope (AFM). The average peak-to-peak surface roughness was about 20 nm with a root-mean-square (rms) deviation of 4 nm. This surface roughness was independent of any of the static deformation described above. The average reflectivity of the polycrystalline silicon surface was measured using a custom-designed interferometer and found to be approximately 40% at an optical wavelength of 633 nm. This measurement suggests that a reflective coating is needed to provide reflectivity and optical efficiency sufficient for use in an adaptive optics system.

III. Residual Stresses

A surface map and cross sectional profile of a 100-actuator continuous mirror array in the unactuated state are shown in Fig. 10.

As in all of the surface maps shown, the vertical axis is highly exaggerated in comparison to the other two axes. A waffle pattern of mirror deflection can be observed, measuring approximately 50 nm peak-to-valley (25-nm rms). The pattern is fairly regular in shape, repeating with a period equal to the actuator spacing. This deformation occurs after structural release of the mirror membrane, and appears, roughly to the same degree, in both segmented and continuous mirror membranes. The likely cause is residual stress gradients in the polycrystalline silicon films. While these deviations from flatness are relatively small compared to the thickness of the mirrors, and represent less than 5% of the usable stroke, they represent significant fractions of the wavelength of visible light, and will, therefore, adversely affect the performance of the mirror in an adaptive optics application. It is important to note that the period of this deformation is equal to the interactuator spacing, so it is not possible to compensate with the mirror's own actuators. The deformation observed in Fig. 10 provides an acceptable optically flat surface, with rms figure error less than 5% of the wavelength. However, reduction in this figure error would be advantageous for optical performance.

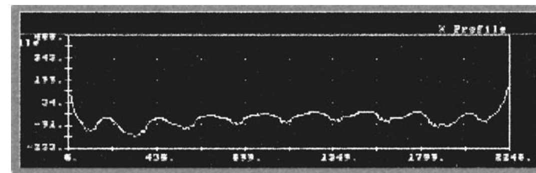

(a)

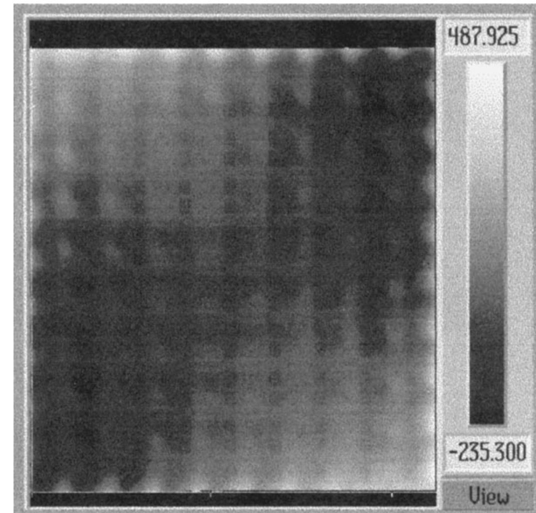

(b)

Fig. 10. (a) Interferometric profile and (b) surface map of unactuated 10 × 10 continuous mirror.

It is possible to compensate for this initial interactuator deformation using a matched phase filter in the optical beam path, provided that the interactuator deformation pattern remains invariant with arbitrary actuation of the mirror membrane. Such optical phase compensation is similar in optical function to the job performed by the deformable mirror itself, but is time invariant and must be achieved with much finer spatial resolution. A simulation of this compensation can be synthesized by subtracting the interferometric map data in Fig. 10 from the data in Fig. 9. The resulting image, shown in Fig. 11, is largely free of the effects of interactuator residual deformation. This type of compensation complicates the already difficult adaptive optics problem, however.

IV. Optical Control Experiments

MEMS mirror devices derived from our custom fabrication process were used to implement a real time, closed loop analog feedback control system capable of dynamic correction of optical aberrations. Fig. 12 shows the experimental setup. A collimated, 4 mW HeNe laser beam was focused via a lens onto a single segment of a tip-tilt MEMS mirror of the type depicted in Fig. 1(c). A dynamic aberration was introduced using warm air turbulence from a candle flame placed beneath the beam path. The spatial wavelength of the aberration was much larger than the beam diameter, hence the effect of the aberration was to introduce a dynamic tilt in the propagation direction of the beam. A "quad cell" photodetector was used to determine the centroid of the reflected beam along two orthogonal axes in the image plane.

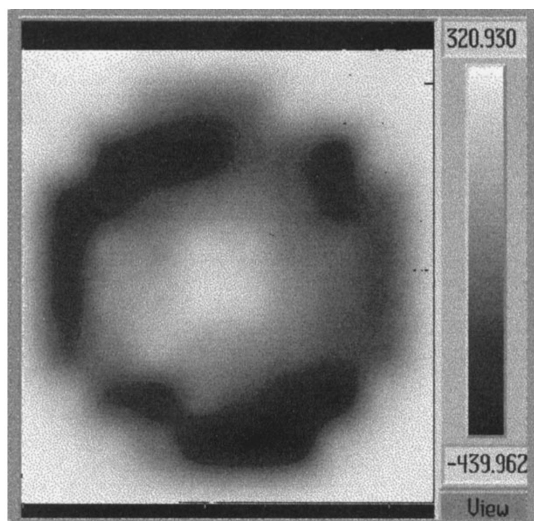

Fig. 11. Surface map obtained by subtracting the reference image (Fig. 10) from the dome image (Fig. 9).

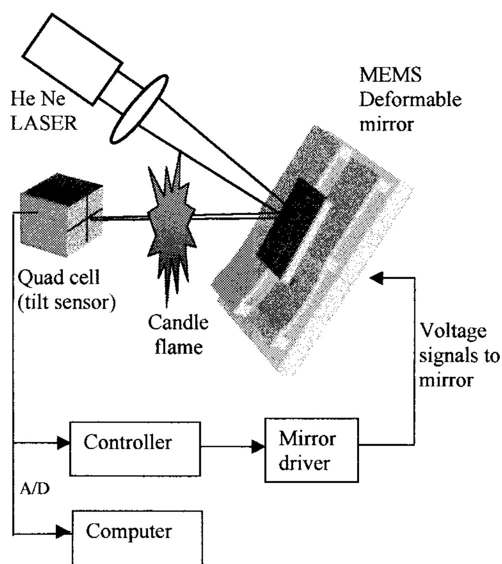

Fig. 12. Schematic of the experimental setup for real time control of tilt aberration.

Each photodiode produces an analog signal proportional to its net received energy flux. The differential signal produced along each axis of the detector corresponds to the location of the centroid of the incident beam. The two outputs from the quad cell (one for each axis) were fed to two closed loop, proportional control feedback circuits. The output of the control circuits were amplified, added to an offset, and used to drive four actuators at the corners of the tip-tilt MEMS mirror segment. Because electrostatic actuators can only be pulled toward the substrate, an offset is required to permit both positive and negative tilt about an initial bias deflection. The sensor output was transformed into digital form using an analog-to-digital (A/D) converter and stored in a computer.

Fig. 13 shows the measured tip and tilt of the laser beam for a 2-kHz sample rate over 5 s. Light gray corresponds to the locus of the beam path with the feedback controller turned off. Black corresponds to locus of the beam path with the feedback controller turned on. Significant reduction in beam

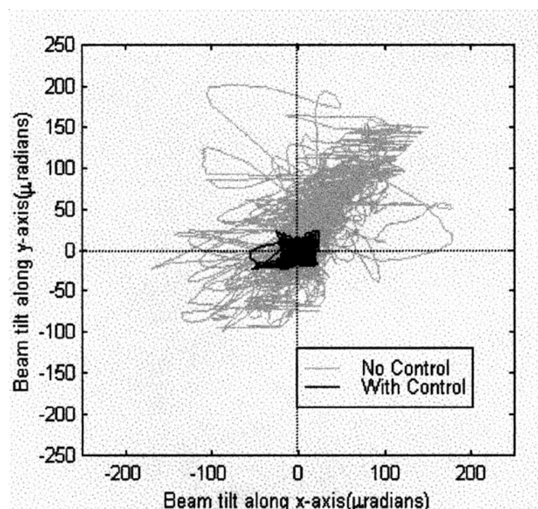

Fig. 13. Two axis beam tilt measured by a quad cell photodetector, demonstrating correction of beam tilt using one segment of a MEMS-DM.

tilt by due to the adaptive optics system is evident with the feedback controller is turned on.

In a final experiment to measure usable bandwidth of mirror devices, an actuator beneath a continuous mirror element was driven by a sinusoidal input over approximately 50% of its actuation range while a high-speed interferometer measured deflection. By sweeping the actuation frequency from dc to 10 kHz, a frequency response curve was generated. For the mirror element tested, the 3-dB rolloff frequency was determined to be 3.5 kHz. This bandwidth would be more than adequate for most adaptive optics applications.

V. Conclusion

The goal of this work was to introduce a MEMS deformable mirror technology that could be used in an adaptive optics system for dynamic phase modulation. Results from prototype devices demonstrate the feasibility of continuous and segmented mirror MEMS-DM's with independently controllable zones. These mirrors exhibit ample stroke (2 μm) for compensation of typical aberrations in visible light. The position repeatability resolution of the system is approximately 10 nm. No hysteresis or temporal drift was observed in any devices, and yield of >95% was routinely achieved in prototype devices. The mirror bandwidth was measured to be dc–3.5 kHz.

The MEMS-DM prototype devices were fabricated using relatively conventional surface micromachining and were driven using low-cost low-power electronics. In total, the cost for fabricating a single prototype system with 100 actuators, mounted and wirebonded in a ceramic package with a PC addressable driver system, was less than $5000.

The electrostatic actuators operate without hysteresis and require about 200 V for operation. Although the actuator itself draws almost no current, the controller drive circuitry draws 100 mW/channel. This is an exceptionally low power system.

The entire package for the prototype mirror is approximately 35 $\times$ 35 $\times$ 6 mm with an active mirror area of 7 mm $\times$ 7 mm for a 400-element MEMS-DM.

The membrane mirror topography in MEMS-DM's is strongly affected by design layout, print through from the actuator thin films, holes needed to release sacrificial layers, and residual stresses in the mirror itself. A design-based strategy to reduce topography and limit etch access holes has proven successful at limiting print through and reducing topography.

The performance exhibited by these prototype MEMS-DM's is promising, though improvements in optical quality and surface planarity are needed.

The advantages of MEMS-DM's in cost, compactness, power consumption, and speed in comparison to existing DM's should, over the next several years, extend the range of optical imaging and beamforming applications that can benefit from adaptive compensation.

ACKNOWLEDGMENT

The authors wish to thank MCNC, Research Triangle Park, NC, where all surface micromachingin was performed.

REFERENCES

[1] G. Vdovin and P. Sarro, "Flexible mirror micromachined in silicon," *Appl. Opt.,* vol. 34, pp. 2968–2972, 1995.

[2] L. M. Miller, M. Argonin, R. Bartman, W. Kaiser, T. Kenny, R. Norton, and E. Vote, "Fabrication and characterization of a micromachined deformable mirror," *Proc. SPIE,* vol. 1945, 1993, pp. 421–430.

[3] M. Roggemann, V. Bright, B. Welsh, S. Hick, P. Roberts, W. Cowan, and J. Comtois, "Use of micro-electro mechanical deformable mirrors to control aberrations in optical systems: Theoretical and experimental results," *Opt. Eng.,* vol. 36, no. 2, pp. 1327–1338, May 1997.

[4] D. Koester, R. Mahadevan, and K. W. Markus, "MUMP's introduction and design rules," tech. paper, MCNC Technology Applications Center, 3021 Cornwallis Road, Research Triangle Park, NC, Oct. 1994.

[5] R. Krishnamoorthy Mali, T. Bifano, M. Horenstein, and N. Vandelli, "Development of microelectromechanical deformable mirrors for phase modulation of light," *Opt. Eng.,* vol. 36, no. 2, pp. 542–548, Feb. 1997.

[6] M. Horenstein, T. Bifano, R. Krishnamoorthy Mali, and N. Vandelli, "Electrostatic effects in micromachined actuators for adaptive optics," *J. Electrostat.,* vol. 42, pp. 1–2, Sept. 1997.

[7] T. Bifano, R. Krishnamoorthy Mali, J. Dorton, J. Perreault, N. Vandelli, M. Horenstein, and D. Castañon, "Continuous membrane, surface micromachined, silicon deformable mirror," *Opt. Eng.,* vol. 36, no. 5, pp. 1354–1360, May 1997.

Thomas G. Bifano received the B.S. and M.S. degrees in mechanical engineering and materials science from Duke University and the Ph.D. degree in mechanical engineering from North Carolina State University.

He is an Associate Professor in the Department of Aerospace and Mechanical Engineering at Boston University, Boston, MA, and President of the Prism Corporation, Boston, MA. His research currently includes development of MEMS array systems for optical mirrors, microfluidic valves, and sonoelectric hydrophones; development of manufacturing technology for compact disc production; use of kinetic ion beams to pattern submicrometer sized features in ceramics and glasses; and basic research on the design, fabrication, and control of smart materials. He has organized and chaired two international conferences for the American Society for Precision Engineering and recently served as a member of the Board of Directors for that society.

Julie Perreault received the B.S. degree in electrical engineering and is an AASERT Graduate Fellow in the Department of Electrical and Computer Engineering, Boston University, Boston, MA.

Her graduate work is directed toward control of optical MEMS array systems and integration of MOEMS in adaptive optics applications.

Raji Krishnamoorthy Mali received the B.S. in mechanical engineering from the University of Bombay, Bombay, India, and the M.S. and Ph.D. degrees in mechanical engineering from Boston University, Boston, MA.

She is currently a Development Engineer for Standard Micro Systems Corporation (SMSC) in Hauppage, NY. During the course of the research described in this paper, she was a Presidential University Graduate Fellow in mechanical engineering at Boston University.

Mark N. Horenstein received the Ph.D. and S.B. degrees from MIT and the M.S. degree from the University of California at Berkeley.

He is an Associate Professor in the Department of Electrical and Computer Engineering at Boston University. He specializes in the fields of electrostatics, electronics, and instrumentation and measurement. His research activities have included the design of a MEMS-based electric field mill sensor, interdigitated capacitive sensors for single-side measurement of MEMS actuator deflection, the design of a high voltage MEMS driver arrays, and the development of switching architectures for addressing of large scale MEMS arrays. He holds several patents related to electrostatic devices and processes. He is the author of *Microelectronics Circuits and Devices*, a widely read book on analog and digital electronics. He is on the Executive Council of the Electrostatics Society of America.